



# Optimized Schwarz waveform relaxation algorithms with nonconforming time discretization for coupling convection-diffusion problems with discontinuous coefficients

Eric Blayo, Laurence Halpern, Caroline Japhet

## ► To cite this version:

Eric Blayo, Laurence Halpern, Caroline Japhet. Optimized Schwarz waveform relaxation algorithms with nonconforming time discretization for coupling convection-diffusion problems with discontinuous coefficients. Olof B. Widlund and Walter Zulehner. Domain Decomposition Methods in Science and Engineering XVI, 55, Springer Verlag, pp.267-274, 2007, Lecture Notes in Computational Science and Engineering, 978-3-540-34468-1. 10.1007/978-3-540-34469-8\_31 . inria-00187555

**HAL Id: inria-00187555**

**<https://inria.hal.science/inria-00187555>**

Submitted on 14 Nov 2007

**HAL** is a multi-disciplinary open access archive for the deposit and dissemination of scientific research documents, whether they are published or not. The documents may come from teaching and research institutions in France or abroad, or from public or private research centers.

L'archive ouverte pluridisciplinaire **HAL**, est destinée au dépôt et à la diffusion de documents scientifiques de niveau recherche, publiés ou non, émanant des établissements d'enseignement et de recherche français ou étrangers, des laboratoires publics ou privés.

---

# Optimized Schwarz waveform relaxation algorithms with nonconforming time discretization for coupling convection-diffusion problems with discontinuous coefficients

Eric Blayo<sup>1</sup>, Laurence Halpern<sup>2</sup>, and Caroline Japhet<sup>2</sup>

<sup>1</sup> LMC, Université Joseph Fourier, B.P. 53, 38041 Grenoble Cedex 9, France  
`Eric.Blayo@imag.fr`

<sup>2</sup> LAGA, Université Paris XIII, 99 Avenue J-B Clément, 93430 Villetaneuse, France  
`halpern@math.univ-paris13.fr`, `japhet@math.univ-paris13.fr`

**Summary.** We present and study an optimized Schwarz Waveform Relaxation algorithm for convection-diffusion problems with discontinuous coefficients. Such analysis is a first step towards the coupling of heterogeneous climatic models. The SWR algorithms are global in time, and thus allow for the use of non conforming space-time discretizations. They are therefore well adapted to coupling models with very different spatial and time scales, as in ocean-atmosphere coupling. As the cost per iteration can be very high, we introduce new transmission conditions in the algorithm which optimize the convergence speed. In order to get higher order schemes in time, we use in each subdomain a discontinuous Galerkin method for the time-discretization. We present numerical results to illustrate this approach, and we analyse numerically the time-discretization error.

## 1 Introduction

We present an optimized Schwarz Waveform Relaxation algorithm for convection-diffusion problems with discontinuous coefficients. Such methods have proven to be an efficient approach in the case of the wave equation with discontinuous wave speed [3], and convection-diffusion problems in one [1] and two dimensions [5] with constant coefficients. Our final objective is to propose efficient algorithms for coupling heterogeneous models (e.g. ocean-atmosphere) in the context of climate modelling. The SWR algorithms are global in time, and therefore are well adapted to coupling models: they lead, at convergence, to a model with the physical transmission conditions, they reduce the exchange of information between codes, and they permit the use of non conforming discretizations in space-time. This last point is crucial in climate modelling, where very different scales in time and space are present.

As a first step, we consider the domain decomposition problem for a convection-diffusion equation with discontinuous coefficients. After introducing our model problem in Section 2, we present in Section 3 a classical strategy for coupling ocean and

atmosphere models, which consists in realizing one additive Schwarz iteration with physical transmission conditions, in each time window [6]. In order to get a more efficient method which improves the converged solution, we introduce in Section 4 a Schwarz Waveform Relaxation method with optimized transmission conditions of order 1. This method allows for the use of non conforming space-time discretizations. As our objective is to get higher order schemes in time, we introduce a discontinuous Galerkin method [4]. The formulation is given in Section 5. As the grids in time are different in each subdomain, the projection between arbitrary grids is performed by an efficient algorithm introduced in [3]. Numerical results illustrate the validity of our approach in Section 6.

## 2 Model problem

We consider the one dimensional convection diffusion equation

$$\begin{aligned} \mathcal{L}u &= f, & \text{in } \Omega \times (0, T), \\ u(x, 0) &= u_0(x), & \forall x \in \Omega, \\ u(x_0, t) &= u(x_1, t) = 0, & t \in (0, T), \end{aligned}$$

where  $\Omega = ]x_0, x_1[$  is a bounded open subset of  $\mathbb{R}$  (containing zero),  $\mathcal{L}$  is the convection diffusion operator

$$\mathcal{L}u := \frac{\partial u}{\partial t} + \frac{\partial}{\partial x}(a(x)u) - \frac{\partial}{\partial x}(\nu(x)\frac{\partial u}{\partial x}),$$

and the velocity  $a$  and the viscosity  $\nu$  are supposed to be constant in the two nonoverlapping subregions  $\Omega_1 = ]x_0, 0[$  and  $\Omega_2 = ]0, x_1[$  of  $\Omega$ , but can be discontinuous at zero :

$$a(x) = \begin{cases} a_1, & x \in \Omega_1 \\ a_2, & x \in \Omega_2 \end{cases}, \quad \nu(x) = \begin{cases} \nu_1, & x \in \Omega_1 \\ \nu_2, & x \in \Omega_2 \end{cases},$$

with  $\nu_i > 0$ ,  $i = 1, 2$ . Without loss of generality, we can assume that  $a$  is non-negative. This problem is equivalent to the following subproblems :

$$\begin{cases} \mathcal{L}_1 u_1 := \frac{\partial u_1}{\partial t} + a_1 \frac{\partial u_1}{\partial x} - \nu_1 \frac{\partial^2 u_1}{\partial x^2} = f, & \text{in } \Omega_1 \times (0, T), \\ u_1(x, 0) = u_0(x), & \forall x \in \Omega_1, \\ u_1(x_0, t) = 0, & t \in (0, T), \end{cases}$$

$$\begin{cases} \mathcal{L}_2 u_2 := \frac{\partial u_2}{\partial t} + a_2 \frac{\partial u_2}{\partial x} - \nu_2 \frac{\partial^2 u_2}{\partial x^2} = f, & \text{in } \Omega_2 \times (0, T), \\ u_2(x, 0) = u_0(x), & \forall x \in \Omega_2, \\ u_2(t, x_1) = 0, & t \in (0, T), \end{cases}$$

with the physical transmission conditions at  $x = 0$  :

$$\begin{cases} u_1(0, t) = u_2(0, t), & t \in (0, T), \\ (a_1 - \nu_1 \frac{\partial}{\partial x})u_1(0, t) = (a_2 - \nu_2 \frac{\partial}{\partial x})u_2(0, t), & t \in (0, T). \end{cases} \quad (1)$$

To solve numerically this problem, it is natural to use an algorithm where the transmission conditions are the physical conditions (in our case, conditions (1)), and it is especially the case when coupling heterogeneous climate component models.

### 3 Algorithm in ocean-atmosphere coupling

A commonly used strategy for solving ocean-atmosphere coupling consists in decomposing the time interval  $(0, T)$  into windows,  $[0, T] = \cup_{n=0}^N [T_n, T_{n+1}]$ , and to use one additive Schwarz iteration with the physical transmission conditions, in each time window [6]. Let  $u_{i,n}$  be a discrete approximation of  $u_i$  in  $\Omega^i$  in the window  $[T_{n-1}, T_n]$ . Then,  $u_{i,n+1}$ ,  $i = 1, 2$ , is the solution of

$$\begin{cases} \mathcal{L}_1 u_{1,n+1} = f, & \text{in } \Omega_1 \times (T_n, T_{n+1}), \\ u_{1,n+1}(x, T_n) = u_{1,n}(x, T_n), & \forall x \in \Omega_1, \\ u_{1,n+1}(x_0, t) = 0, & t \in (T_n, T_{n+1}), \\ u_{1,n+1}(0, t) = u_{2,n}(0, T_n), & t \in (T_n, T_{n+1}), \end{cases} \quad (2)$$

$$\begin{cases} \mathcal{L}_2 u_{2,n+1} = f, & \text{in } \Omega_2 \times (T_n, T_{n+1}), \\ u_{2,n+1}(x, T_n) = u_{2,n}(x, T_n), & \forall x \in \Omega_2, \\ u_{2,n+1}(t, x_1) = 0, & t \in (T_n, T_{n+1}), \\ (a_2 - \nu_2 \frac{\partial}{\partial x}) u_{2,n+1}(0, t) = (a_1 - \nu_1 \frac{\partial}{\partial x}) u_{1,n}(0, T_n), & t \in (T_n, T_{n+1}), \end{cases} \quad (3)$$

*Remark 1.* It is important to notice that in the previous algorithm the transmission conditions are constant in time, on each time window  $(T_i, T_{i+1})$ .

In ocean-atmosphere coupling, the use of very few iteration (one iteration here) in each time window is motivated by the fact that the computation time per iteration is very high. In order to improve the numerical solution, with very few iteration per time window, we propose to use in each time window an Optimized Schwarz Waveform Relaxation, with differential in time transmission conditions.

### 4 Optimized Schwarz Waveform Relaxation

The general Schwarz Waveform Relaxation, in one time window, for example in the whole window  $(0, T)$  is written as follows :

$$\begin{cases} \mathcal{L}_1 u_1^{k+1} = f, & \text{in } \Omega_1 \times (0, T), \\ u_1^{k+1}(x, 0) = u_0(x), & \forall x \in \Omega_1, \\ u_1^{k+1}(x_0, t) = 0, & t \in (0, T), \\ (\nu_1 \frac{\partial}{\partial x} - a_1 + \Lambda_1) u_1^{k+1}(0, t) = (\nu_2 \frac{\partial}{\partial x} - a_2 + \Lambda_1) u_2^k(0, t), & t \in (0, T), \end{cases}$$

$$\begin{cases} \mathcal{L}_2 u_2^{k+1} = f, & \text{in } \Omega_2 \times (0, T), \\ u_2^{k+1}(x, 0) = u_0(x), & \forall x \in \Omega_2, \\ u_2^{k+1}(t, x_1) = 0, & t \in (0, T), \\ (\nu_2 \frac{\partial}{\partial x} - a_2 + \Lambda_2) u_2^{k+1}(0, t) = (\nu_1 \frac{\partial}{\partial x} - a_1 + \Lambda_2) u_1^k(0, t), & t \in (0, T), \end{cases}$$

where  $\Lambda_1$  and  $\Lambda_2$  are linear operators, involving derivatives in time.

### 4.1 Optimized transmission conditions

The optimal transmission conditions can be derived from a Fourier analysis in the case  $\Omega = \mathbb{R}$ . Using the error equations and a Fourier transform with parameter  $\omega$ ,

$$\rho(\omega) := \left( \frac{\lambda_2(\omega) - r_1^-(\omega)}{\lambda_1(\omega) - r_1^-(\omega)} \right) \left( \frac{\lambda_1(\omega) - r_2^+(\omega)}{\lambda_2(\omega) - r_2^+(\omega)} \right)$$

with  $r_1^-(\omega) = \frac{a_1 - \sqrt{a_1^2 + 4\nu_1 i \omega}}{2}$ ,  $r_2^+(\omega) = \frac{a_2 + \sqrt{a_2^2 + 4\nu_2 i \omega}}{2}$  and  $\lambda_i, i = 1, 2$  the symbol of  $A_i$ . The optimal choice, which gives a convergence in 2 iterations, is  $\lambda_2 = r_1^-(\omega)$  and  $\lambda_1 = r_2^+(\omega)$ . The calculations are straightforward extensions to those in [1]. As the optimal corresponding transfer operators  $A_1, A_2$  are nonlocal in time and thus more costly than local transfers, we propose to use the following transfer operators

$$A_1 := \frac{a_2 + p_2}{2} + \frac{q_2}{2} \frac{\partial}{\partial t}, \quad A_2 := \frac{a_1 - p_1}{2} - \frac{q_1}{2} \frac{\partial}{\partial t}$$

where the parameters  $p_1, p_2, q_1, q_2$  minimize the convergence rate. The condition on the parameters  $p_1, p_2, q_1, q_2$  for the local subdomain problems to be well-posed are  $q_j \geq 0$  (due to energy estimates as in [1]). The question of convergence of the algorithm remains open, even though there are numerical evidences for a positive answer (see [2] for theoretical results using Robin transmission conditions).

### 4.2 Optimized Schwarz Waveform Relaxation with time windows

We now define the algorithm with many several time windows : Let  $[0, T] = \cup_{n=0}^N [T_n, T_{n+1}]$ , and let  $p \geq 1$  be an integer, that we will take small (typically  $p \leq 3$ ) in order to make very few iterations in each time window. Let  $u_{i,n}^k$  be a discrete approximation of  $u_i$  in  $\Omega^i$  in the window  $(T_{n-1}, T_n)$  at step  $k$  of the SWR method. Then, the next time window's solution  $u_{i,n+1}$  in  $\Omega^i$  is obtained after  $p$  SWR iterations :

for  $k = 0, \dots, p-1$  :

$$\left\{ \begin{array}{ll} \mathcal{L}_1 u_{1,n}^{k+1} = f, & \text{in } \Omega_1 \times (T_n, T_{n+1}), \\ u_{1,n}^{k+1}(x, T_n) = u_{1,n}(x, T_n), & \forall x \in \Omega_1, \\ u_{1,n}^{k+1}(x_0, t) = 0, & t \in (T_n, T_{n+1}), \\ (\nu_1 \frac{\partial}{\partial x} - a_1 + A_1) u_{1,n}^{k+1}(0, t) = (\nu_2 \frac{\partial}{\partial x} - a_2 + A_1) u_{2,n}^k(0, t), & t \in (T_n, T_{n+1}), \end{array} \right. \quad (4)$$

$$\left\{ \begin{array}{ll} \mathcal{L}_2 u_{2,n}^{k+1} = f, & \text{in } \Omega_2 \times (T_n, T_{n+1}), \\ u_{2,n}^{k+1}(x, T_n) = u_{2,n}(x, T_n), & \forall x \in \Omega_2, \\ u_{2,n}^{k+1}(t, x_1) = 0, & t \in (T_n, T_{n+1}), \\ (\nu_2 \frac{\partial}{\partial x} - a_2 + A_2) u_{2,n}^{k+1}(0, t) = (\nu_1 \frac{\partial}{\partial x} - a_1 + A_2) u_{1,n}^k(0, t), & t \in (T_n, T_{n+1}), \end{array} \right. \quad (5)$$

and  $u_{1,n+1} := u_{1,n}^p$ ,  $u_{2,n+1} := u_{2,n}^p$ .

## 5 Time discretization with a discontinuous Galerkin Method

Let us introduce the discretization of the subproblems in a time window  $I = (T_n, T_{n+1})$ . We consider, for example, the subproblem in  $\Omega_1$  at step  $k$  of the SWR procedure. It can be written in the form

$$\begin{cases} \mathcal{L}_1 u = f & \text{in } \Omega_1 \times I, \\ u(x_0, \cdot) = 0 & \text{in } I, \\ (\nu_1 \frac{\partial u}{\partial x} + \beta u + \gamma \frac{\partial u}{\partial t})(0, \cdot) = g & \text{in } I, \\ u(\cdot, 0) = u_0, & \text{in } \Omega_1, \end{cases}$$

with  $\beta = -a_1 + \frac{a_2 + p_2}{2}$ ,  $\gamma = \frac{q_2}{2}$ , and  $g(t) = (\nu_2 \frac{\partial}{\partial x} - a_2 + A_1)u_{2,n}^k(0, t)$ .

This problem is equivalent to the weak formulation : Find  $u(t) \in V = H^1(\Omega_1)$  such that  $u(0) = u_0$  and

$$((\dot{u}(t), v)) + \tilde{a}(u(t), v) = \ell_t(v), \quad \forall v \in V$$

with  $(\cdot, \cdot)$  the scalar product in  $L^2(\Omega_1)$ , and for  $u \in V$  :

$$\begin{cases} ((u, v)) := (u, v) + \gamma u(0)v(0) \\ \tilde{a}(u, v) := b(u, v) + \beta u(0)v(0), \quad \text{with } b(u, v) = \nu_1 (\frac{\partial u}{\partial x}, \frac{\partial v}{\partial x}) + a_1 (\frac{\partial u}{\partial x}, v) \\ \ell_t(v) := (f(t), v) + g(t)v(0) \end{cases}$$

The discontinuous Galerkin Method [4] is based on the use of a discontinuous finite element formulation in time. Let  $I = \prod_{k=1}^K I_k$  with  $I_k = [t_{k-1}, t_k]$ , and let  $v_+^k = \lim_{s \rightarrow 0^+} v(t_k + s)$  and  $v_-^k = \lim_{s \rightarrow 0^-} v(t_k + s)$ . Let  $V_h$  be a finite-dimensional subspace of  $V$ , and

$$\mathbb{P}_q(I_k) = \{v : I_k \longrightarrow V_h : v(t) = \sum_{i=0}^q v_i t^i \text{ with } v_i \in V_h\}$$

The discontinuous Galerkin Method can now be formulated as follows :

$$\begin{cases} U_-^0 = u_0 \\ \text{For } k = 1, \dots, K, \text{ given } U_-^{k-1}, \text{ find } U \equiv U|_{I_k} \in \mathbb{P}_q(I_k) \text{ such that} \\ \int_{I_k} [((\dot{U}, v)) + \tilde{a}(U, v)] dt + ((U_+^{k-1}, v_+^{k-1})) = \\ \int_{I_k} \ell_t(v) dt + ((U_-^{k-1}, v_+^{k-1})), \quad \forall v \in \mathbb{P}_q(I_k) \end{cases} \quad (6)$$

For  $q = 0$ , using the notations  $U^k \equiv U_-^k \equiv U_+^{k-1}$  and  $\Delta t_k = t_k - t_{k-1}$ , the method reduces to

$$\begin{cases} U^0 = u_0 \\ \text{For } k = 1, \dots, K, \text{ find } U^k \in V_h \text{ such that} \\ ((\frac{U^k - U^{k-1}}{\Delta t_k}, v)) + \tilde{a}(U^k, v) = \frac{1}{\Delta t_k} \int_{I_k} \ell_t(v), \quad \forall v \in V_h \end{cases}$$

This method is a simple modification of the backward Euler scheme in that case.

For  $q = 1$ , (6) is equivalent to the following system with, for  $t \in I_k$ ,  $U(t) = U_0 + \frac{t - t_{k-1}}{\Delta t_k} U_1$ ,  $U_i \in V_h$ ,

$$\left\{ \begin{array}{l} (U_0, v) + \Delta t_k b(U_0, v) + (\Delta t_k \beta + \gamma) U_0(0) v(0) + (U_1, v) + \frac{1}{2} \Delta t_k b(U_1, v) \\ \quad + \Delta t_k \left( \frac{\beta}{2} + \gamma \right) U_1(0) v(0) = (U_-^{k-1}, v) + \gamma U_-^{k-1}(0) v(0) \\ \quad \quad \quad + \int_{I_k} (f(s), v) ds + v(0) \int_{I_k} g(s) ds, \quad \forall v \in V_h \\ \\ \frac{1}{2} \Delta t_k b(U_0, v) + \frac{\beta}{2} \Delta t_k U_0(0) v(0) + \frac{1}{2} (U_1, v) + \frac{1}{3} \Delta t_k b(U_1, v) \\ \quad + \left( \frac{\gamma}{2} + \frac{\beta}{3} \Delta t_k \right) U_1(0) v(0) = \frac{1}{\Delta t_k} \int_{I_k} (s - t_{k-1}) (f(s), v) ds \\ \quad \quad \quad + \frac{1}{\nu_1} v(0) \int_{I_k} (s - t_{k-1}) g(s) ds, \quad \forall v \in V_h \end{array} \right.$$

## 6 Numerical results

In this presentation, we take  $q = 0$  in the discontinuous Galerkin method.

### 6.1 Relative $L^2$ error versus the time step

In this part, we consider the case with one time window only, with different grids in time in each subdomain, and we observe the relative  $L^2$  error between the SWR converged solution and the continuous solution, versus the number of refinements of the time grid. We choose  $a_1 = a_2 = 1$ ,  $\nu_1 = \nu_2 = 1$ , and  $u(x, t) = \sin(x)\cos(t)$ , in  $[0, 2\pi] \times [0, 2.5]$  as exact solution. The space domain  $[0, 2\pi]$  is decomposed in two subdomains  $\Omega_1 = [0, 2]$  and  $\Omega_2 = [2, 2\pi]$ . The mesh size is  $h_1 = 0.01$  for  $\Omega_1$  and  $h_2 = (2\pi - 2)/200$  for  $\Omega_2$ . In order to compare the  $L^2$  relative error on the nonconforming time grids case to the error obtained on a uniform conforming time grid, we consider four initial meshes in time (see figure 1) :

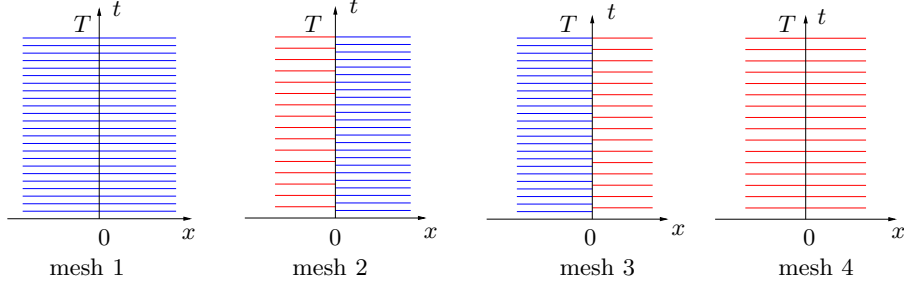
- a uniform finer conforming mesh (mesh 1) with  $\Delta t = 2.5/24$ ,
- a nonconforming mesh (mesh 2) with  $\Delta t = 2.5/24$  in  $\Omega_1$  and  $\Delta t = 2.5/16$  in  $\Omega_2$ ,
- a nonconforming mesh (mesh 3) with  $\Delta t = 2.5/16$  in  $\Omega_1$  and  $\Delta t = 2.5/24$  in  $\Omega_2$ ,
- a uniform coarser conforming mesh (mesh 4) with  $\Delta t = 2.5/16$ .

Figure 2 shows the relative  $L^2$  error versus the number of refinement for these four meshes, and the time step  $\Delta t$  versus the number of refinement, in logarithmic scale. At each refinement, the time step is divided by two. The results of Figure 2 show that the relative  $L^2$  error tends to zero at the same rate than the time step, and this fits with the error estimates in [4]. On the other hand, we observe that the two curves corresponding to the nonconforming meshes (mesh 2 and mesh 3) are between the curves of the conforming meshes (mesh 1 and mesh 4).

### 6.2 Comparison of the 2 algorithms

In this part, we consider the problem

$$\begin{cases} \mathcal{L}u = 0 & \text{in } ]0, 6[ \times ]0, 3[ \\ u(0, t) = u(6, t) = 0, t \in [0, 3], & u(x, 0) = e^{-3(1.2-x)^2}, x \in [0, 6] \end{cases}$$



**Fig. 1.** Uniform conforming time grids (mesh 1 and mesh 4) and nonconforming time grids (mesh 2 and mesh 3)

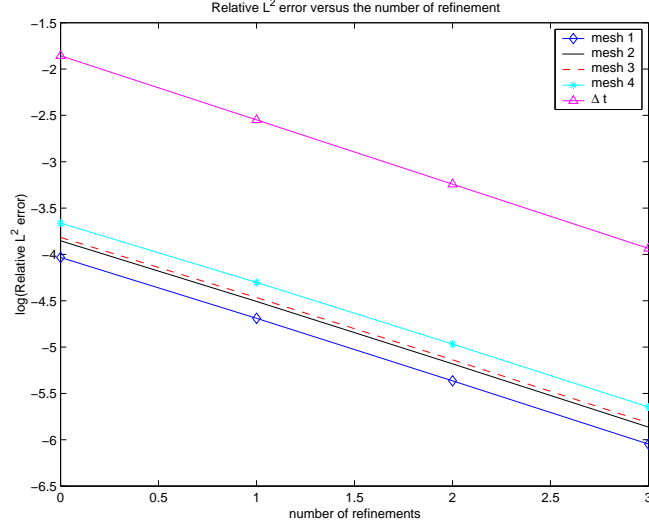


**Fig. 2.** Relative  $L^2$  error versus the number of refinements for the initial meshes : mesh 1 (diamond line), mesh 2 (solid line), mesh 3 (dashed line), and mesh 4 (star line). The triangle line is the time step  $\Delta t$  versus the number of refinements, in logarithmic scale.

In order to compare algorithm (2)-(3) to the SWR algorithm (4)-(5), we decompose the time interval into three windows :  $[0, 3] = [0, 1] \cup [1, 2] \cup [2, 3]$  and we compare the computed solutions obtained from each method. We take  $a_1 = 0.1$ ,  $\nu_1 = 0.2$ ,  $a_2 = \nu_2 = 1$ . The space domain  $[0, 6]$  is decomposed in two subdomains  $\bar{\Omega}_1 = [0, 3]$  and  $\bar{\Omega}_2 = [3, 6]$ . The mesh size is  $h_1 = 0.01$  for  $\Omega_1$  and  $h_2 = 0.06$  for  $\Omega_2$ . The time step in each window is  $\Delta t_1 = 0.01$  for  $\Omega_1$  and  $\Delta t_2 = 0.02$  for  $\Omega_2$ . On figure 3 on the right, we observe that the 3-windows computed solution with the SWR algorithm (4)-(5) is close to the one-window solution. Moreover it more precise than the 3-windows computed solution of figure 3 which is obtain with the algorithm (2)-(3) (figure 3 on the left).



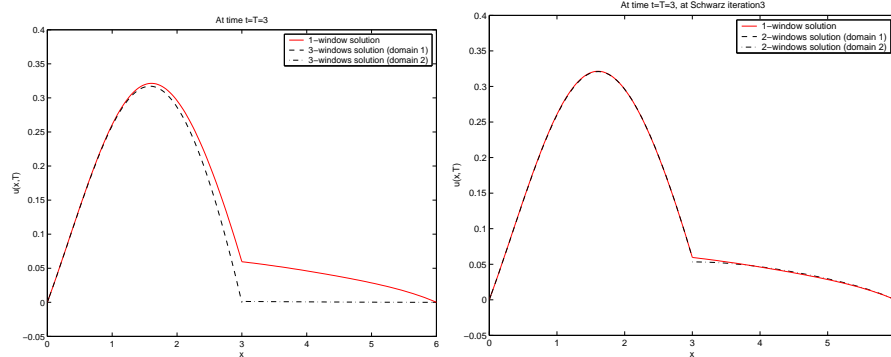


**Fig. 3.** One time window solution (solid line) and 3-windows solutions (dashed line for  $\Omega_1$  and dashdot line for  $\Omega_2$ ), with algorithm (2)-(3) on the left, at time  $t=T=3$ , and with the SWR method on the right, at time  $t=T=3$ , and at SWR iteration 3.

## 7 Conclusion

We have introduced a Schwarz Waveform Relaxation Algorithm for the convection-diffusion equation with discontinuous coefficients. The transmission conditions involve normal derivatives and derivatives in time as well. We have used those in computations, together with a zero-order discontinuous Galerkin method and a projection between the time grids. We showed numerically that the discretization order is preserved. We intend now to extend the strategy to higher order Galerkin methods, and to write projection steps that keep, for the whole process, the order of the scheme in each subdomain.

## References

1. D. Bennequin, M. Gander, and L. Halpern. Optimized Schwarz waveform relaxation for convection reaction diffusion problems. Technical Report 24, LAGA, Université Paris 13, 2004.
2. M. Gander, L. Halpern, and M. Kern. Schwarz waveform relaxation method for advection-diffusion-reaction problems with discontinuous coefficients and non-matching grids. In *This volume*. dd16, 2005.
3. M. Gander, L. Halpern, and F. Nataf. Optimized Schwarz waveform relaxation method for the one dimensional wave equation. *SIAM Journal on Num. Anal.*, 41(5), 2003.
4. C. Johnson. *Numerical solution of partial differential equations by the finite element method*. Cambridge University Press, New York, 1987.
5. V. Martin. An optimized Schwarz waveform relaxation method for unsteady convection diffusion equation. *Applied Num. Math.*, 52(4):401–428, 2005.
6. P. Pellerin, H. Ritchie, F. Saucier, F. Roy, S. Desjardins, M. Valin, and V. Lee. Impact of a two-way coupling between an atmospheric and an ocean-ice model over the gulf of St. Lawrence. *Monthly Weather Review*, 32:1379–1398, 2004.